Modelling of wide frequency range silicon microphone for acoustic measurement

D. Ekeom, Libor Rufer

▶ **To cite this version:**

D. Ekeom, Libor Rufer. Modelling of wide frequency range silicon microphone for acoustic measurement. Acoustics 2012, Apr 2012, Nantes, France. hal-00772366

HAL Id: hal-00772366
https://hal.science/hal-00772366

Submitted on 10 Jan 2013

HAL is a multi-disciplinary open access archive for the deposit and dissemination of scientific research documents, whether they are published or not. The documents may come from teaching and research institutions in France or abroad, or from public or private research centers.

L'archive ouverte pluridisciplinaire **HAL**, est destinée au dépôt et à la diffusion de documents scientifiques de niveau recherche, publiés ou non, émanant des établissements d'enseignement et de recherche français ou étrangers, des laboratoires publics ou privés.

Modelling of wide frequency range silicon microphone for acoustic measurement

D. Ekeom[a] and L. Rufer[b]

[a]Microsonics, 39, rue des Granges galand, 37550 Sain-Avertin, France
[b]TIMA Laboratory, 46, rue Félix Viallet, 38031 Grenoble, France
didace.ekeom@microsonics.fr

Résumé

Ce travail démontre à l'aide de simulations numériques, la faisabilité d'un microphone piézorésistif de large gamme de fréquence et de haute pression acoustique basé sur la technologie MEMS. Un modèle réduit précis a été utilisé pour optimiser la réponse dynamique du microphone. Les paramètres mécaniques réduits ont été extraits à partir des simulations structurelles FEM, alors que les paramètres de la couche d'air ont été extraits d'une simulation par éléments finis de l'équation linéarisée de Reynolds. Finalement, les paramètres acoustiques de rayonnement ont été extraits à partir d'un couplage éléments finis-éléments de frontière.
Des microphones avec des membranes rectangulaires et circulaires, vibrant en mode de flexion et suspendues par quatre bras ont été simulés. Dans les deux cas, nous avons été en mesure d'atteindre les spécifications requises pour les applications aéro-acoustiques: une réponse en fréquence plate jusqu'à 980 kHz et une sensibilité d'environ 10.5 µV/Pa. Le bruit électrique et le quotient signal sur bruit thermomécanique étaient de 6.4 µV/Pa et 67 dB respectivement.

Abstract

This work demonstrates with numerical simulations, the feasibility of a wide frequency range and high pressure level piezoresistive microphone based on MEMS technology. An accurate lumped-element model was used to optimize the microphone dynamic response. Mechanical lumped parameters were extracted from structural finite element method (FEM) simulations, while squeeze film fluid parameters were extracted from FEM simulation of linearized Reynolds's equation. Finally, acoustic radiation parameters were extracted from a weak coupling between the FEM and the boundary element method (BEM).
Microphones with rectangular and circular membrane, vibrating in bending mode and suspended by four beams were simulated. In both cases we were able to achieve the specifications required for aero-acoustic applications: A flat frequency response up to 980 kHz and a sensitivity of about 10.5 µV/Pa. The electrical noise and mechanical thermal signal to noise ratio were 6.4 µV/Pa and 67 dB respectively.

Keywords: Silicon microphone, Wide frequency band, Lumped-element model, Finite element method.

1 Introduction

Microphones are transducers that convert acoustic pressure into electrical signal [1]. The main transduction principles that have been developed for MEMS devices are capacitive, piezoelectric and piezoresistive. Capacitive microphones are made of a diaphragm (called here as a membrane) and a fixed electrode. Such a structure forming a variable capacitor is biased with an electrical field and activated by acoustic pressure. Due to the acoustic pressure, the vibration of the membrane induces the capacitance change, which generates an electrical output signal. The main difficulty to design a high frequency capacitive microphone consists in the small value of the capacitance due to the small size of the membrane active area. Typical specifications of capacitive MEMS microphones are a sensitivity of 10 µV/Pa to 50 mV/Pa and a frequency range of 10 Hz to 200 kHz. Piezoelectric MEMS microphones consist of a thin membrane that is either covered with piezoelectric material or mechanically linked with a piezoelectric bender. The vibration of the membrane induces stress in the piezoelectric material, which generates an electrical output signal. Typical specifications of piezoelectric MEMS microphones are a sensitivity of 20 mV/Pa to 40 mV/Pa and a frequency range of 10 Hz to 20 kHz [2]. The main obstacles for the use of piezoelectric principle for the design of high frequency microphones are in the relatively high level of the electric noise, low sensitivity, and the high value of the electrical impedance.

These specifications are inadequate for aero-acoustic applications, such as characterization of "N-waves" generated by supersonic flights that require microphones with wide frequency range (from 10 kHz to 1 MHz), with flat response and high-pressure levels (up to 4 kPa). A piezoresistive microphone consists of a membrane provided with one or several piezoresistors. Typically, two or four piezoresitors are integrated in a Wheatstone bridge. The strain due to the pressure induced deformation of the membrane results in the change of the piezoresistor resistance, which generates an electrical output signal. The main advantage of a piezoresitive microphone is the relatively low output impedance.

This work demonstrates, with numerical simulations, the feasibility of a wide frequency range and a high pressure level piezoresistive microphone for aero-acoustic applications based on MEMS technology. Section II presents an accurate lumped-element model of the microphone. It was developed and used to optimize the microphone dynamic response. Mechanical lumped parameters were extracted from structural FEM simulations, while squeeze film fluid parameters were extracted from FEM simulation of linearized Reynolds's equation. Finally, acoustic radiation parameters were extracted from a weak coupling between the FEM and the BEM. Section III deals with microphone design. Microphones with either square or circular perforated membranes, suspended by four beams, vibrating in bending mode and damped with a squeezed film of fluid were simulated. The obtained results match the aero-acoustic requirements.

2 Numerical model

This section deals with lumped-element model simulation of a piezoresistive microphone dynamic response. Special attention was paid to the lumped-element model parameters identification. The active part of the microphone (perforated membrane, beams and piezoresistive resistors) was governed by the elastostatic and elastodynamic equations. The external fluid domain (above the microphone) was governed by Helmholtz equation [3]. Finally the squeeze film fluid was governed by compressible Reynolds's equation [4]. For an accurate simulation, these three physical fields must be coupled. Thus, the mechanical and fluidic problems were simulated with FEM (Ansys) [5], while the acoustic radiation was simulated with the BEM (Microsonics) [6]. Lumped-element model parameters were extracted and the full system was weakly coupled in order to simulate the dynamic response of the microphone, as an equivalent spring-mass-damper system under harmonic excitation (Figure 1). The associated motion equation is given by Eq. (1).

$$m\frac{d^2u(t)}{dt^2}+c\frac{du(t)}{dt}+k\ u(t)=F(t) \qquad (1)$$

Where m, c and k are the effective mass, damping coefficient, and stiffness, respectively.

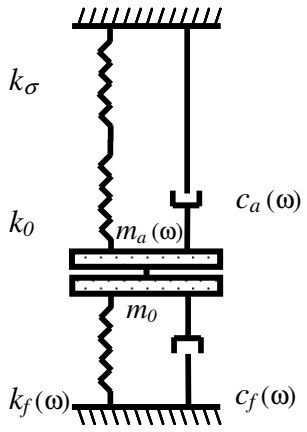

Figure 1: Microphone lumped-element model.

The global coefficients m, c, and k are composed of several parts. k_0, and m_0 are the mechanical stiffness and the effective mass of the active part, free of residual stress. We assume that the effective mass of the active part do not change with the residual stress. k_σ is the mechanical stiffness due to residual stress. $c_a(\omega)$ and $m_a(\omega)$ are the acoustic radiation damping coefficient and the radiation mass. $k_f(\omega)$ and $c_f(\omega)$ are the stiffness and damping coefficients of the squeeze film. The global effective stiffness $k = k_0 + k_\sigma + k_f(\omega)$, the global effective damping coefficient $c = c_a(\omega) + c_f(\omega)$ and finally, the global effective mass $m = m_0 + m_a(\omega)$. ω is the angular pulsation. Note that the thermoelastic damping and the viscous damping of the structure were neglected. The interaction with the substrate was also neglected. The lumped-element model parameters identification procedure is presented in detail here after.

1. A static analysis of the structure was performed. The beams were clamped and a unit pressure (1 Pa) was applied on the active part. The residual stress in the membrane was set to zero. From the deformed structure, the mechanical strain energy of the active part and the displacement quadratic average u^2 were obtained. Then, the mechanical stiffness k_0, was estimated as:

$$\frac{1}{2}k_0u^2=\frac{1}{2}\int_\Omega \sigma:\varepsilon\ d\Omega \qquad (2)$$

Where the right hand side of Eq. (2) is the mechanical strain energy of the membrane active part. It is obtained by integrating the stress-strain tensor product. The symbols σ and ε correspond to stress and strain tensors. The average value of the strain in the piezoresistor was evaluated. Combined with the gauge factor, it leads to the relative resistor variation $\Delta R/R$ for applied pressure of 1 Pa.

2. A first modal analysis of the membrane with clamping beams, free of residual stress, was performed. The frequency f_0 of the first mode (bending mode) was extracted. The effective mass of the structure m_0 was estimated with the aid of Eq. (3).

$$f_0=\frac{1}{2\pi}\sqrt{\frac{k_0}{m_0}} \qquad (3)$$

3. A second modal analysis of the same structure but considering the residual stress was performed. The frequency f_σ of the first mode (bending mode) was extracted. The mechanical stiffness including the residual stress effect was obtained by means of Eq. (4). The residual stress is assumes to be in-plane.

$$f_\sigma=\frac{1}{2\pi}\sqrt{\frac{k_0+k_\sigma}{m_0}} \qquad (4)$$

4. The pressure distribution in the squeeze film (air-gap) was governed by linearized compressible Reynolds's equation [4]. The following assumptions were made. (*i*) No external force acts on the film fluid. (*ii*) The structure oscillates with small amplitude and the main flow is derived by pressure gradient in the lateral directions. (*iii*) The flow is laminar, isothermal and rarefaction effects were taken into account by means of the Knudsen number. The harmonic analysis of the linearized compressible Reynolds's equation was conducted under the following boundary conditions. A uniform velocity v was applied on the active part; ambient pressure was applied at the open edges of the active part and at the top of the ventilation holes. The pressure distribution was computed and the stiffness coefficient of the squeeze film $k_f(\omega)$ and the damping coefficient $c_f(\omega)$ were evaluated with Eq. (5) and Eq.(6), respectively.

$$k_f(\omega)=\int_\Gamma \frac{\omega P_I(r,\omega)}{v}d\Gamma_r \qquad (5)$$

$$c_f(\omega)=\int_\Gamma \frac{P_R(r,\omega)}{v}d\Gamma_r \qquad (6)$$

Where $P_R(r,\omega)$ and $P_I(r,\omega)$ are the real and imaginary parts of the pressure, Γ is the active area. The spring and damping forces were deduced as $k_f(\omega)\ v/\omega$ and $c_f(\omega)\ v$ respectively.

5. To take into account the acoustic radiation in the semi-infinite fluid medium, the acoustic half-space BEM formulation was used. Developed over a century ago [6], this formulation provides a simple but exact representation for radiation from a flat vibrating surface mounted on an infinite rigid baffle. Because of a very high impedance shift between the structure and the surrounding air, a weak FEM-BEM coupling was used. First, a harmonic analysis of the structure was performed. The output velocity on the structure was used as the boundary condition for the BEM simulation. The extracted pressure was used to evaluate the acoustic radiation impedance Eq. (7) [3].

$$Z(\omega) = \frac{\int_\Gamma p(r,\omega)\ \ v^*(r,\omega)\ \ d\Gamma_r}{\int_\Gamma v(r,\omega)\ \ v^*(r,\omega)\ \ d\Gamma_r} \qquad (7)$$

The augmented (radiation) mass and damping coefficient due to acoustic radiation, $m_a(\omega)$ and $c_a(\omega)$ were deduced from the acoustic radiation impedance with Eq. (8) and Eq.(9).

$$m_a(\omega) = \frac{S\ Z_I(\omega)}{\omega} \qquad (8)$$

$$c_a(\omega) = S\ Z_R(\omega) \qquad (9)$$

Where, S is the area of the structure active part, Z_R and Z_I are the real and imaginary parts of the acoustic radiation impedance.

3 Microphone design

The developed lumped-element model was used to design wide frequency range piezoresistive microphones. The microphones were constituted either with square or circular membranes. The membranes were perforated with nine ventilation holes of 5 µm diameter each and suspended over the air gap with fours beams. The membrane and the four beams were made of 1 µm thick silicon nitride layer. Its material properties used for the simulations are as follows: $\rho = 2200$ kg/m^3, $E = 270$ GPa, $\upsilon = 0.27$, $\sigma = 200$ MPa. Where, ρ is the density, E is the Young modulus, ν is the Poisson ratio and σ is the in-plane residual stress. The piezoresistors were located close to the clamped end of each beam. They were made of 0.2 µm thick metal-induced laterally crystallized polycrystalline silicon, because such a fabrication technique guarantees good piezoresistive response characteristics [7]. Its elastic material properties used for the simulations were: $\rho = 2300$ kg/m^3, $E = 150$ GPa, $\upsilon = 0.22$. The Knudsen number of the squeeze film fluid was estimated as $K_n = (L_0\ P_{ref}) / (P_0\ H)$. Where $L_0 = 64\ 10^{-3}$ µm/s is the mean free path length of the fluid. P_{ref} is the reference pressure for the mean free path, P_0 is the ambient pressure. In the work P_{ref} and P_0 are equals to 105 kPa. H is the thickness the squeeze film fluid (air gap). The dynamic viscosity of squeeze film was $\eta = 18.3\ 10^{-12}$ kg/(µm s). The density and speed velocity of the outside fluid used in the simulation were 1.20 kg/m^3 and 343. m/s respectively. Figure 2 presents schematic top views of the simulated microphones.

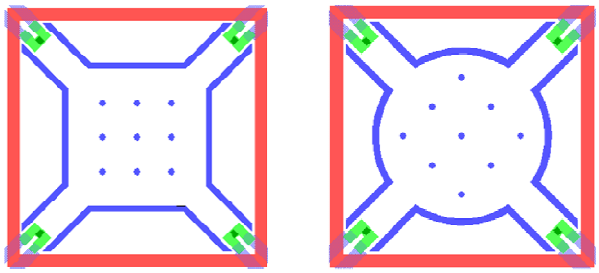

Figure 2: Simulated microphones.

The microphones geometrical specifications are presented in Table I. T is the thickness of the membrane and the beams. A is the characteristic dimension of the membrane (length for the square membrane or diameter for the circular membrane), it was chosen so that the active parts with square and circular membrane have the same area. L and W are the length and width of the beams respectively, H is the air gap thickness.

Table I: Geometry specifications.

Shape	T (µm)	A (µm)	L (µm)	W (µm)	H (µm)
Square	1	120	60	25	1.45
Circular	1	135.4	60	25	1.60

In the following work, the gauge factor of the piezoresistors was supposed to be equal to 40 and the input voltage of the Wheatstone bridge was supposed to be 2.5 V. The static and modal analysis of the structure combined with Eq.(2) and Eq.(3), lead to the lumped-element parameters of the structures (Table II). Note that the frequencies f_σ corresponding to the first bending mode were around 520 kHz while the frequencies of the second mode were above 1410 kHz. Thus, we can assume that the two modes do not interact each other and that the microphone is free of parasitic modes in the desired frequency range.

Table II: Mechanical lumped parameters.

Shape	k_0+k_σ(µN/µm)	m_0 (ng)	f_σ(kHz)
Square	411.7	38.71	519
Circular	427.8	39.81	522

Static performances of the microphone are summarized at Table III. P_{min} is the lowest value of pressure that can be

detected. It was estimated with the assumption that the electrical noise of an associated electronics has a level of about 25 µV. P_{max} is the highest value of pressure that can be supported by the structure without any damage. It was estimated with the assumption that the displacement at the centre should be smaller than $H/3$. P_{dis} is the value of a pressure for which a distortion appears in the signal. We assume that the disturbing distortion appears when the displacement at the centre of the membrane is about $H/10$. This assumption was made because the squeeze film spring and damping forces versus frequency curves exhibit a noticeable change when the air gap thickness variation exceeds 10%.

Table III: Static performance of microphones.

Shape	$\Delta R/R$ (ppm/Pa)	P_{min} (Pa)	P_{dis} (Pa)	P_{max} (Pa)
Square	4.45	2.24	1476	2399
Circular	4.22	2.37	1732	3316

The main microphone dynamic parameters are summarized in Tables IV and V. f_1 and f_2 are the first and second mechanical resonance frequencies of the structure vibrating in vacuum, when residual stress are taken into consideration. Therefore $f_1 = f_\sigma$. $BW_{-3\,dB}$ and $BW_{-6\,dB}$ are the bandwidth at -3 dB and at -6 dB, respectively. $f_{cut\text{-}off}$ is the squeeze film fluid cut-off frequency. S_v is the electrical sensitivity, R is the electrical resistance of the piezoresistor, V_{elec} the electrical noise and SNR is the thermal-mechanical signal to noise ratio.

Table IV: Frequencies and bandwidth (*).

Shape	f_1	$BW_{-3\,dB}$	$BW_{-6\,dB}$	$f_{cut\text{-}off}$	f_2
Square	519	820	970	1345	1416
Circular	522	850	985	1210	1411

(*) all units of Table IV are in kHz.

Table V: Dynamic performance of microphones.

Shape	S_v (µV/Pa)	R (Ω)	V_{elec} (µV)	SNR (dB)
Square	11.12	3066	6.339	67.46
Circular	10.55	3066	6.456	67.40

Figure 3 shows the spring and damping forces of the squeeze film fluid versus frequency, acting on the active part. Squeeze film cut-off frequency is defined as the frequency for which spring and damping forces are equal. Figure 4 shows the electrical dynamic response of the microphone (magnitude and phase) versus frequency.

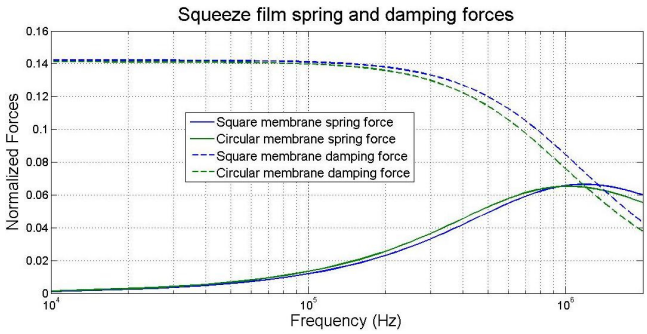

Figure 3: Spring and damping force versus frequency.

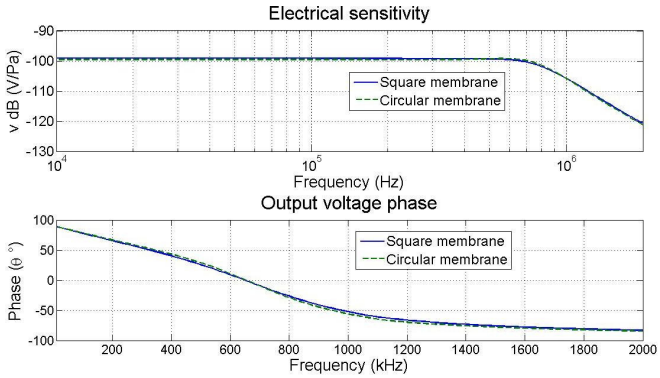

Figure 4: Dynamic response of microphone.

Three-dimensional numerical simulations of piezoresistive microphones with square and circular membranes but of equivalent active areas, with equivalent ventilation holes distribution and of same beams length were conducted. Lumped-element model parameters were extracted and microphones specifications were estimated. Results and main differences between microphones with rectangular and circular membranes are discussed hereafter:

i) Results of Table III indicate that pressure level for which disturbing distortion appears in the electrical dynamic signal is greatly higher for the microphone with circular membrane. This is the consequence of a higher mechanical stiffness and higher air gap thickness. The higher mechanical stiffness of the circular membrane comparing to the square one leads to a lower electrical sensitivity of the corresponding microphone (Table V), with equivalent electrical resistance of the piezoresistors, electrical noise and mechanical thermal signal to noise ratio. Note that the lowest pressure that can be measured is quite similar for both kinds of microphones.

ii) Table IV shows that for both microphones, the second mechanical resonant frequency f_2 is approximately three times higher than the first mechanical resonance frequency f_1, which is associated to the operational bending mode of the microphones. On the other hand, the second mechanical resonance frequency f_2 is considerably higher than the cut-off frequency of the squeeze film fluid. Thus, we can assume that the microphones are free of parasitic modes, that can disturb their dynamics responses.

iii) The two microphones exhibit flat electrical dynamic responses (magnitude of the electrical sensitivity on Figure 4) up to 850 kHz, while the electrical sensitivity phase exhibits a linear response up to 1 MHz. Dynamic electrical responses of both types of microphones are very similar. This is due to the fact that the most of lumped parameters used for the simulation are equivalent.

4 Conclusion

A lumped-element model of a piezoresistive microphone was developed. Special attention was given to the lumped parameters extraction procedure. This procedure was based on finite element method for structural and fluidic analysis and boundary element method for the acoustic analysis. The multiphysics solution was coupled as a spring-mass-damper system under a harmonic excitation. The developed lumped-model was used to design two piezoresistive microphones with square and circular membranes. The obtained specifications were: wide frequency response up to 980 kHz, electrical sensitivity of about 10.5 µV/Pa and maximal pressure level up to 1.7 kPa. The electrical noise and mechanical thermal signal to noise ratio were 6.4 µV/Pa and 67 dB respectively. These specifications satisfy requirements of aero-acoustic microphone designated for measurements on models of sonic boom propagation. Our future work will focus on the fabrication and characterization of the designed microphone.

ACKNOLEDGEMENT

The work has been done with the support of the French National Research Agency (ANR) Program BLANC 2010 SIMI 9 for the project SIMMIC and the European Fund for Economic and Regional Development (FEDER). The authors want to thank Zhijian Z. Zhou from the Hong Kong University of Science and Technology, for fructuous discussions and support.

References

[1] P. R. Scheeper, A. G. H. Van Der Donkb, W. Olthuis and P. Bergveld, "A review of silicon microphones", Sensors and Actuators A 44, pp. 1-11, (1994).

[2] Tian-Ling Ren, Lin-Tao Zhang, Jian-She Liu, Li-Tian Liu, Zhi-Jian Li, A novel ferroelectric based microphone, Microelectronic Engineering 66, pp. 683–687, (2003).

[3] A. D. Pierce, "Acoustic, introduction to its physical principles and applications", Mc Graw-Hill Book company, (1981).

[4] R. Pratap, S. Mohite and A. K. Pandey, "Squeeze film effects in MEMS devices", Journal of the Indian Institute of science, vol. 87:1, pp. 75- 94, (2007).

[5] ANSYS version 13.0, user's guide, ANSYS Inc., Pittsburgh, (2010).

[6] A. F. Seybert and T. K. Rengarajan, “The high frequency radiation of sound from bodies of arbitrary shape”, J. Vib. Acoust. Stress Reliab. Des., ASME transaction, vol. 109, pp. 381-387, (1987).

[7] M. Wang, Z. Meng, Y. Zohar and M. Wong, "Metal-induced laterally crystallized polycrystalline silicon for integrated sensor applications," Electron Devices, IEEE Transactions on, vol. 48, pp. 794-800, (2001).